Previous Paper Back to Programme Back to Topic Next Paper

A Thermomechanical Constitutive Model for Fibrous Reinforcements

J.J. Cheng[a], P.A. Kelly[a], S. Bickerton[b]
[a]Department of Engineering Science, School of Engineering
[b]Department of Mechanical Engineering, Center for Advanced Composite Materials,
The University of Auckland, Private Bag 92019, Auckland 1142, New Zealand
j.cheng@auckland.ac.nz

SUMMARY

In Liquid Composite Moulding processes, many important manufacturing parameters and final properties of the part are influenced by the constitutive behaviour of fibrous reinforcements. A thermomechanical model for the response of fibrous materials to compaction is presented. Rate-dependent and rate-independent features observed in experimental data are reproduced by the model.

Keywords: compaction, fibrous materials, permanent deformation, viscoelastic, thermomechanical

INTRODUCTION

Liquid Composite Moulding (LCM) is an all-encompassing term for composite material manufacturing processes such as Resin Transfer Moulding (RTM), Compression Resin Transfer Moulding (CRTM) and Vacuum Assisted Resin Infusion (VARI). LCM processes allow one to form parts of small to large scale, having complex geometries and varying fibre reinforcement layup patterns. The potential for lower cost processing via LCM has led to the increasing adoption of LCM processes within the aerospace, automotive and other industries.

The development of a model for preform compaction described in this paper is part of a larger project to produce a full scale simulation of a generic LCM process. As such, one requires a compaction model which is accurate, capable of capturing the salient features evident in experimental data and simple to characterise. Furthermore, the computational expense of the model should not be prohibitively high.

To date, several micromechanical approaches to modelling fibrous material behaviour have been carried out. In 1946, van Wyk [1] likened a fibrous material to a random assembly of fibres in contact with one another, forming a collection of *bending units* between contact points, each governed by elementary beam theory. A relationship between the average length of bending segments and total volume of the assembly was derived, leading to a non-linear power relation between applied compaction stress and fibre volume fraction. Rate dependent phenomena and permanent deformation are not accounted for. Other authors have also used this probability-based approach, extending the work to account for the fibre orientation distribution [2-4] and the inclusion of inelastic effects [5]. In the latter, a rate-independent hysteretic response is produced.

On complete unloading, some strain energy remains locked in the fibres as a consequence of a fibre-fibre friction mechanism [5].

The works mentioned thus far do not explicitly account for the microstructure within the tow. On the scale of fibres forming a single tow, Cai and Gutowski [6] considered a bundle of lubricated aligned fibres and presented a model exhibiting non-linear elasticity and viscous effects. This work was extended by Simacek and Karbhari [7], considering dry unlubricated aligned bundles, for which modes of permanent deformation were considered.

Other micromechanical models employ an approach involving *unit cells* or *representative volume elements*, in which geometric details at the meso-scale, treating tows as solid bodies, are represented explicitly. This is particularly useful in the case of knitted or woven fabrics [8-11]. Whilst details such as the yarn cross sectional shape are used in the prediction of the material response, these models do not reproduce the permanent deformation or rate-dependent effects present in experimental data, as this most likely requires interactions within the yarn to be considered. At present, the computational expense of simulating the many thousands of individual fibres within the tow contacting and sliding against each other appears prohibitively high, particularly in a full-scale LCM simulation.

An alternative approach to the micromechanical one involves a treatment of fibrous materials as continua. Standard continuum mechanics permits the consideration of inelastic effects and is less computationally expensive than micromechanical models. Models built from a combination of individually simple spring, dashpot and friction-block elements have successfully reproduced the permanent deformation and rate-dependent response typical of fibrous materials [12-15]. The application of classical plasticity theory and standard viscoplastic models has also produced promising results. [16]

The thermomechanical model proposed in this paper utilises a continuum approach, but lies within a framework which ensures that thermodynamic requirements are satisfied. Physical phenomena contributing to the material behaviour are postulated and defined through the evolution of *state variables*, which is additionally governed by the laws of thermodynamics. In this way, physical aspects of micromechanical behaviour are incorporated into a continuum-based framework. The resulting thermomechanical model thus inherits the physical basis of micromechanical approaches and the simplicity and low computational cost of continuum based models.

The complexity of the constitutive response of fibrous materials is well documented. Diversity arises from the vast number of fibre architectures and fibre types available. Features common to the behaviour of most samples include non-linearity, permanent deformation and rate effects, the latter two giving rise to a hysteretic load-unload curve. In addition, a *debulking* response is observed, whereby the material response evolves with cyclic loading.

Robitaille [17] performed a series of experiments on woven fabrics. Debulking effects were observed, whereby the volume fraction following each successive load cycle tended towards a steady state value. Equivalently, Somashekar [18] observed decay in the sample height with cycle number. This was accompanied by decay in the peak compaction stress. The permanent deformation as a percentage of the total deformation was also observed to decrease as compaction speed was increased.

To illustrate the importance of modelling the hysteretic, rate dependent behaviour of fibrous preforms, consider the following LCM processes;

In VARI, a first application of vacuum compacts the fibres. Then, resin flow relieves the effective stress on the preform, leading to unloading of the fibres. Furthermore, during post-filling, a re-loading occurs. The preform is also often debulked through vacuum being drawn and released repeatedly prior to resin infusion.

Similarly, in hard mould processes, the complex behaviour of the preform is necessary to accurately predict tooling forces. Particularly in RTMLight, for which flexible moulds are applied, tool deformations during processing are dependent on mould rigidity and the complex behaviour of the preform and cannot be predicted accurately using a single history-independent loading curve.

Clearly, a single loading curve is inadequate for accurate simulation of the processes mentioned above, underpinning the need for an accurate model which accounts for the complex behaviour of the preform.

THERMOMECHANICAL MODELLING OF FIBROUS MATERIALS

A thermodynamic framework for irreversible, isothermal processes such as that outlined in [19] is used, wherein one has the following thermomechanical statement:

$$\sigma : d = \dot{\Psi} + \Phi \tag{1}$$

σ and d are the stress and deformation rate tensors respectively, their inner product being the internal stress power. The material behaviour is defined by two potentials; Ψ, the Helmholtz free energy potential and Φ, the dissipation rate. Simply put, Ψ is a measure of energy stored within the material, whilst Φ is the rate at which energy is lost from the material to its surroundings (through heat transfer) and is non-negative by the second law of thermodynamics.

As compared to classical models in plasticity, use of the thermomechanical framework is advantageous as it does not require at the outset the definition of relations such as the yield function or flow rule. Indeed, these relations follow directly from knowledge of the energy and dissipation potentials.

Fibrous materials

There are a number of physical processes that may be postulated to determine the general deformation response of fibrous materials.

As first proposed by van Wyk [1], the bending of fibres stores energy. As noted by Carnaby [5], this energy may become *frozen* into the fibre assembly. One could imagine fibres becoming *locked* into bent configurations during compression. As this frozen energy is associated with permanent deformation of the material, it may not be recovered without reversal of the permanent deformation.

Fibres exhibit frictional behaviour, providing an avenue for energy dissipation. Moreover, this frictional behaviour may determine certain aspects of the fibre locking mechanism mentioned previously.

Viscoelastic, or rate-dependent effects, may arise from dissipative time-dependent rearrangement of fibres within tows, varying with the degree of load applied and the loading history.

A SIMPLE 1-DIMENSIONAL MODEL

Consider a one-dimensional model with a single internal variable. Inelastic effects are attributed to evolution of the internal variable, so one equates the internal variable to the inelastic strain using the following decomposition:

$$\varepsilon = \varepsilon^e + \varepsilon^i \qquad \varepsilon^e = \varepsilon - \alpha \qquad \varepsilon^i = \alpha \tag{2}$$

Furthermore, one assumes that the material is *uncoupled*, so that the elastic modulus is independent of the value of the inelastic strain. Thus, the free energy potential takes the form:

$$\Psi(\varepsilon,\alpha) = \Psi_1(\varepsilon-\alpha) + \Psi_2(\alpha) \quad \text{or equivalently,} \quad \Psi(\varepsilon,\alpha) = \Psi_1(\varepsilon^e) + \Psi_2(\varepsilon^i) \tag{3}$$

It is evident that the term Ψ_2 represents energy storage associated with inelastic strain, or frozen energy within the material due to fibres locked in bent configurations.

The dissipation rate is sub-divided into two terms, representing rate-independent and rate-dependent inelastic effects.

$$\Phi = \Phi_1 + \Phi_2 = \frac{\partial \Phi_1}{\partial \dot{\alpha}}\dot{\alpha} + \frac{1}{2}\frac{\partial \Phi_2}{\partial \dot{\alpha}}\dot{\alpha} \tag{4}$$

Φ_1 and Φ_2 are homogeneous functions of degree 1 and 2 respectively in the inelastic strain rate $\dot{\alpha}$.

Substituting the free energy (3) and dissipation (4) potentials into the isothermal thermomechanical statement (1), one obtains the following thermodynamic constraint:

$$0 = \left(\frac{\partial \Psi}{\partial \varepsilon} - \sigma\right)\dot{\varepsilon} + \left(\frac{\partial \Psi}{\partial \alpha} + \frac{\partial \Phi_1}{\partial \dot{\alpha}} + \frac{1}{2}\frac{\partial \Phi_2}{\partial \dot{\alpha}}\right)\dot{\alpha}\ , \tag{5}$$

from which the following relations are deduced:

$$\sigma = \frac{\partial \Psi}{\partial \varepsilon} = \Psi_1'(\varepsilon - \alpha)$$

$$(-\bar{\chi} + \chi_1 + \chi_1)\dot{\alpha} = 0 \tag{6}$$

$$\bar{\chi} = -\frac{\partial \Psi}{\partial \alpha} = \Psi_1'(\varepsilon-\alpha) - \Psi_2'(\alpha) \qquad \chi_1 = \frac{\partial \Phi_1}{\partial \dot{\alpha}} \qquad \chi_2 = \frac{1}{2}\frac{\partial \Phi_2}{\partial \dot{\alpha}}\ ,$$

where $\bar{\chi}$ is termed the quasi-conservative generalized stress and χ_1 and χ_2 are the dissipative generalised stresses for rate-independent and rate-dependent dissipative processes respectively. The term $\Psi_2'(\alpha)$ is also referred to as the *shift stress* $\rho(\alpha)$ in theories of kinematic hardening, as it represents translation of the yield surface in generalized stress space, due to an evolution in the inelastic strain α.

Furthermore, the first equation in (6) can be expressed in rate form, where it is evident that the elastic modulus derives directly from the Ψ_1 term of the free energy potential.

$$\dot{\sigma} = \frac{\partial}{\partial t}\Psi_1' = K^e(\varepsilon,\alpha)\dot{\varepsilon} + K^\alpha(\varepsilon,\alpha)\dot{\alpha}$$

$$K^e(\varepsilon,\alpha) = \Psi_1''(\varepsilon-\alpha) \quad K^\alpha(\varepsilon,\alpha) = -\Psi_1''(\varepsilon-\alpha) \tag{7}$$

Examining the second equation of (6), the equation is necessarily satisfied for elastic deformations, for which $\dot{\alpha} = 0$ by definition. For inelastic processes ($\dot{\alpha} \neq 0$), the following relation between the shift stress and generalized dissipative stresses holds:

$$-\bar{\chi} + \chi_1 + \chi_1 = 0 \tag{8}$$

Note that in the progression from equation (6) to equation (8) the generalized dissipative stresses are not necessarily independent of $\dot{\alpha}$; use has been made of Ziegler's Orthogonality Hypothesis. [20]

The specific forms of the free energy and dissipation potentials are chosen as shown below:

$$\begin{aligned} \Psi_1(\varepsilon - \alpha) &= \frac{1}{m} E(\varepsilon - \alpha)^m \qquad & \Psi_2(\alpha) &= \frac{1}{p} H\alpha^p \\ \Phi_1 &= \operatorname{sgn}(\dot{\alpha})[f\sigma^q + k(\alpha)]\dot{\alpha} \qquad & \Phi_2 &= \eta\dot{\alpha}^2 \end{aligned} \tag{9}$$

The power-law form of Ψ_1 imparts a non-linear elastic response, as is typical for fibrous materials. Ψ_2 accounts for the storage of frozen energy. The dissipation functions are necessarily non-negative and hence comply with the second law of thermodynamics.

Evaluating the associated thermodynamic forces for the free energy potential and the generalised dissipative stresses for the dissipation rate, one has:

$$\begin{gathered} \sigma = E(\varepsilon - \alpha)^{m-1} \qquad \bar{\chi} = \sigma - \rho(\alpha) \qquad \rho(\alpha) = H\alpha^{p-1} \\ \chi_1 = \operatorname{sgn}(\dot{\alpha})[f\sigma^q + k(\alpha)] \qquad \chi_2 = \eta\dot{\alpha}\ , \end{gathered} \tag{10}$$

from which it is clear that the choice of dissipation functions yields frictional and rate dependent dissipative behaviour. The presence of the function $k(\alpha)$ accounts for the non-zero frictional forces within fibrous materials under zero load, as proposed by Carnaby and Pan [5]. This withdrawal stress is assumed to increase with the extent of inelastic strain. In this formulation, a simple linear function of the inelastic strain was chosen.

The relation governing inelastic behaviour (8) may be rewritten as:

$$\sigma - \rho(\alpha) - \operatorname{sgn}(\dot{\alpha})[f\sigma^q + k(\alpha)] - \eta\dot{\alpha} = 0\ , \tag{11}$$

giving rise to the evolution equation for the inelastic strain:

$$\dot{\alpha} = \frac{\sigma - \rho(\alpha) - \operatorname{sgn}(\dot{\alpha})[f\sigma^q + k(\alpha)]}{\eta} \tag{12}$$

Equations (7) and (12) together define the constitutive response of the material in incremental form.

Since from (11), $\operatorname{sgn}(\dot{\alpha})$ is equivalent to $\operatorname{sgn}\big(\sigma - \rho(\alpha)\big)$ for inelastic processes. The evolution equation for $\dot{\alpha}$ in (12) can be more conveniently expressed as:

$$\dot{\alpha} = \frac{\sigma - \rho(\alpha) - \operatorname{sgn}\big(\sigma - \rho(\alpha)\big)[f\sigma^q + k(\alpha)]}{\eta}$$

$$\operatorname{sgn}(\dot{\alpha}) = \operatorname{sgn}\big(\sigma - \rho(\alpha)\big) \qquad (13)$$

Conditions for which the two equations cannot be simultaneously satisfied imply elastic loading is taking place.

RESULTS AND DISCUSSION

In this section, the proposed thermomechanical model is implemented in a simple compaction simulation to reproduce the features observed in typical experiments on fibrous materials. Trends associated with changes in compaction speed and the cyclic evolution in maximum compaction stress and residual inelastic deformation are reproduced using the model.

Single Cycle

In the experiments by Somashekar [21], square 200mm by 200mm Continuous Filament Random Mat (CFRM), Plain Weave Fabric (PWF) and Biaxial Stitched Fabric (BSF) glass reinforcement specimens were loaded to a target volume fraction, held, then quickly released.

Table 1: Single cycle compaction experiment details [18]

CFRM Target final / initial v_f	Compaction speed (mm/min)	Sample layers	Strain hold time (min)
0.40 / 0.05	1	10	10
0.40 / 0.05	5	10	10
0.40 / 0.05	25	10	10

The normalised peak compaction stresses and inelastic deformation recorded for the experiments [21] are compared with output from the thermomechanical model in Figure 1. Table 2 shows the parameters used in the model.

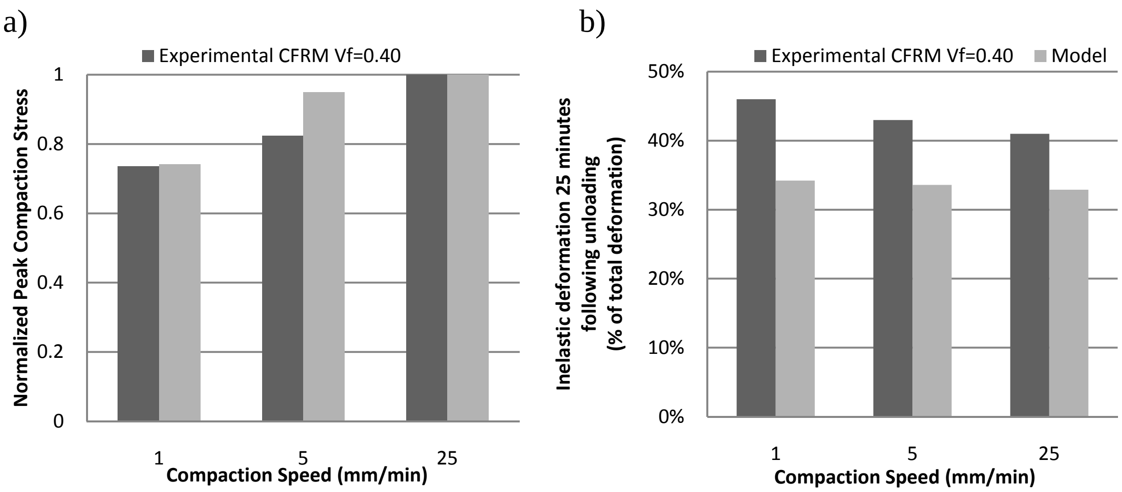

Figure 1: Single cycle compaction
a) Normalised Peak Compaction Stress vs. Compaction Speed, and b) Inelastic deformation 25 minutes after load cycle vs. Compaction Speed

Table 2: Model Parameters

Ψ_1	E	2.00e4
	m	8
Ψ_2	H	E/10
	p	5
Φ_1	f	0.1
	q	1.5
	$k(\alpha)$	0.1 α
Φ_2	η	100000

As shown in the Figure 1, the model exhibits the same rate-dependent trends as observed in experiments, suggesting the validity of the underlying physical processes proposed. As compaction speed is increased, there is less time within which the time-dependent process of fibre rearrangement within the tows may occur. Consequently, the extent to which fibre slippage may occur is reduced. Due to reduced settlement of the material, the elastic strain to which the material is subjected is increased, leading to an increased Peak Compaction Stress.

The frictional resistance to slippage is a non-linear function of the applied stress implying the existence of a *fibre bound* state, wherein the material can no longer deform inelastically due to the frictional dissipative stress χ_1 exceeding the applied stress.

From Figure 1b it is evident that the model underestimates the extent of inelastic deformation 25 minutes after the loading cycle. This result is characteristic of the model, which predicts an eventual steady-state value of the inelastic deformation which is somewhat independent of the loading history. Indeed, as long as the inelastic strain has at some point in the loading history exceeded a critical value determined by the fibre withdrawal stress function $k(\alpha)$, the true permanent deformation predicted by the model will tend towards a single, history-independent value. Despite this predisposition, the slight trend exhibited in Figure 1b can be produced through the use of a high viscosity parameter, corresponding to a high reluctance for the fibres within the tow to rearrange and slowing the reversal of inelastic strain through fibre slippage. Thus, the model exhibits greater correlation to the experimentally observed post-loading inelastic strain for shorter time scales.

Multiple Cycles

In more experiments by Somashekar [21], samples of the same size as used for the single cycle experiments were loaded using the same crosshead speed during loading and unloading. 20 loading and unloading cycles were carried out – experiment details are shown in Table 3. Other experiments were carried out at the Centre for Advanced Composite Materials (CACM), Auckland, where Chopped Strand Mat was compacted at a speed of 0.05mm/min to a final volume fraction of 0.425. Figure 3 provides a comparison between experimental data and the model output for the first cycle, and illustrates the cyclic softening behaviour which is characteristic of the model.

Table 3: Multiple cycle compaction experiment details

CFRM	Compaction speed (mm/min)	Strain hold time (min)	Sample recovery time after each compaction and release (min
Target final / initial v_f			
0.40 / 0.05	1	10	5

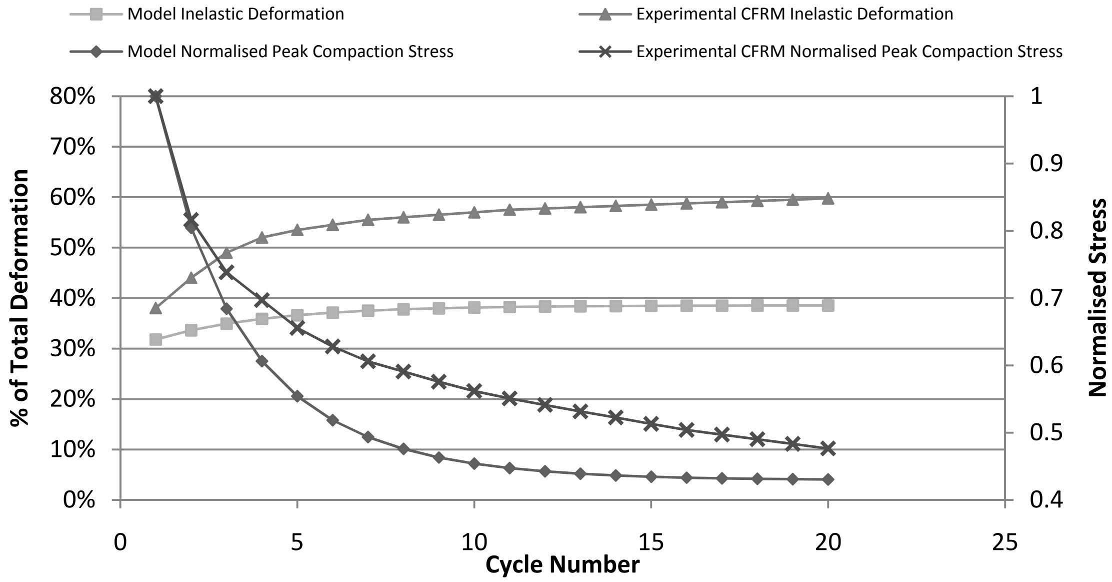

Figure 2: Multiple Cycle Compaction - Inelastic Deformation following each cycle and Normalised Peak Compaction Stress vs. Cycle Number

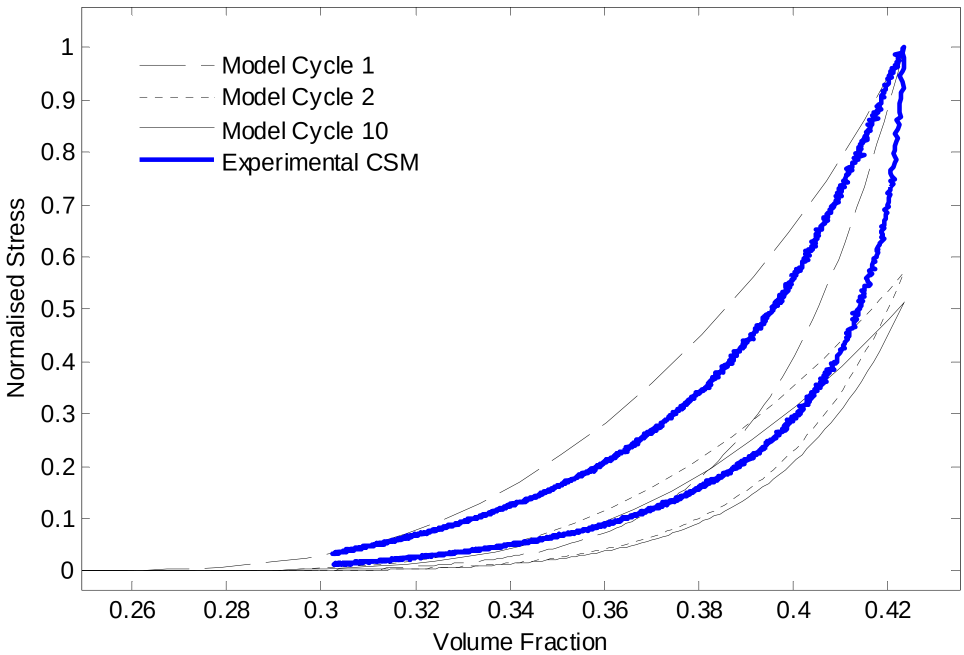

Figure 3: Chopped Strand Mat single cycle experimental data and Model cyclic data – Normalised stress vs. Volume Fraction

The model results in Figure 2 for evolution in inelastic strain from cycle to cycle are qualitatively similar to those observed by Somashekar. A debulking effect is present in both, where the inelastic strain approaches a steady-state value after repeated compaction cycles. The normalized peak compaction stress predicted by the model also shows agreement with the experimentally observed trend. The decay in stress is consistent with the evolution in inelastic strain, in effect reducing the elastic strain applied to the material.

Also in Figure 2, the inelastic deformation predicted by the model is noticeably lower than that observed in experiments. Although the model parameters may be chosen such that this disparity is reduced, it is difficult not to induce other undesirable behaviour, such as excessive stress relaxation, at the same time.

The difficulty in prescribing parameters which allow the model to match the inelastic strain and relaxation behaviour simultaneously lies within the use of a single internal variable, which implies a strong relationship between the physical processes which occur at the intra-tow and inter-tow scales. In reality, these physical processes are distinct, and so would be better described through the use of separate internal variables.

The performance of the model hence illustrates the limitations associated with the use of a single internal variable. Although using a single internal variable keeps the model simple, it is not possible to incorporate an explicit distinction between inelastic fibre slippage and the degree to which intra-tow rearrangement has occurred. This distinction is crucial to an accurate description of fibrous materials, as it allows one to have two samples of the same material having the same inelastic strain, but in different states, due to unique loading histories.

Figure 3 shows experimental data for a single load-unload cycle of a Chopped Strand Mat sample, with model data for cyclic loading overlaid. The model shows general agreement with the experimental data for the first cycle, and the curves for cycles 2 and 10 demonstrate the cyclic softening towards a state of repeatable behaviour that is expected of fibrous materials. A more detailed experimental regime is required in order to make more meaningful comparisons between experiments and the model.

CONCLUSIONS

A thermomechanical model for fibrous materials has been presented. Micro-scale processes of energy storage, by bending of fibres and locking of fibres into bent configurations, and energy dissipation, by fibre slippage and fibre rearrangement within the tow, are represented within the chosen forms of the free energy and dissipation functions. The model has been compared to experimental data for single and multiple cycles of loading. In both instances, the model reproduced the same trends as those observed in the experiments. Suggested improvements to the model include the introduction of an additional internal variable, enabling the physical processes occurring at the inter-tow and intra-tow scales to be treated separately.

ACKNOWLEDGEMENTS

The first author wishes to acknowledge the Royal Society of New Zealand for the provision of a Travel Grant towards attendance at ICCM17.

References

[1] C. M. van Wyk, "Note on the Compressibility of Wool," *Journal of Textile Institute*, vol. 37, pp. T285-T292, 1946.

[2] T. Komori and M. Itoh, "A Modified Theory of Fibre Contact in General Fiber Assemblies," *Textile Research Journal*, vol. 64, pp. 519-528, Sep 1994.
[3] A. E. Stearn, "Effect of Anisotropy in Randomness of Fibre Orientation on Fibre-to-fibre Contacts," *Journal of the Textile Institute*, vol. 62, pp. 353-&, 1971.
[4] D. H. Lee and G. A. Carnaby, "Compressional Energy of the Random Fiber Assembly .1. Theory," *Textile Research Journal*, vol. 62, pp. 185-191, Apr 1992.
[5] G. A. Carnaby and N. Pan, "Theory of the Compression Hysteresis of Fibrous Assemblies," *Textile Research Journal*, vol. 59, pp. 275-284, May 1989.
[6] Z. Cai and T. Gutowski, "The 3-D Deformation-Behavior of a Lubricated Fiber Bundle," *Journal of Composite Materials*, vol. 26, pp. 1207-1237, 1992.
[7] P. Simacek and V. M. Karbhari, "Notes on the modeling of preform compaction .1. Micromechanics at the fiber bundle level," *Journal of Reinforced Plastics and Composites*, vol. 15, pp. 86-122, Jan 1996.
[8] B. X. Chen and T. W. Chou, "Compaction of woven-fabric preforms: nesting and multi-layer reformation," *Composites Science and Technology*, vol. 60, pp. 2223-2231, Sep-Oct 2000.
[9] G. L. Batch, S. Cumiskey, and C. W. Macosko, "Compaction of fiber reinforcements," *Polymer Composites*, vol. 23, pp. 307-318, Jun 2002.
[10] H. Lin, M. Sherburn, J. Crookston, A. C. Long, M. J. Clifford, and I. A. Jones, "Finite element modelling of fabric compression," *Modelling and Simulation in Materials Science and Engineering*, vol. 16, pp. -, Apr 2008.
[11] S. V. Lomov, D. S. Ivanov, I. Verpoest, M. Zako, T. Kurashiki, H. Nakai, and S. Hirosawa, "Meso-FE modelling of textile composites: Road map, data flow and algorithms," *Composites Science and Technology*, vol. 67, pp. 1870-1891, Jul 2007.
[12] Z. Cai, "A Nonlinear Viscoelastic Model for Describing the Deformation-Behavior of Braided Fiber Seals," *Textile Research Journal*, vol. 65, pp. 461-470, Aug 1995.
[13] P. A. Kelly, "A Compaction Model for Liquid Composite Moulding Fibrous Materials," in *The 9th International Conference on Flow Processes in Composite Materials*, Montreal, Canada, 2008.
[14] P. A. Kelly, R. Umer, and S. Bickerton, "Viscoelastic response of dry and wet fibrous materials during infusion processes," *Composites Part a-Applied Science and Manufacturing*, vol. 37, pp. 868-873, 2006.
[15] J. Breard, Y. Henzel, F. Trochu, and R. Gauvin, "Analysis of dynamic flows through porous media. Part II: Deformation of a double-scale fibrous reinforcement," *Polymer Composites*, vol. 24, pp. 409-421, Jun 2003.
[16] V. Lobosco and V. Kaul, "An elastic/viscoplastic model of the fibre network stress in wet pressing: Part 1," *Nordic Pulp & Paper Research Journal*, vol. 16, pp. 12-17, 2001.
[17] F. Robitaille and R. Gauvin, "Compaction of textile reinforcements for composites manufacturing. I: Review of experimental results," *Polymer Composites*, vol. 19, pp. 198-216, Apr 1998.
[18] A. A. Somashekar, S. Bickerton, and D. Bhattacharyya, "An experimental investigation of non-elastic deformation of fibrous reinforcements in composites manufacturing," *Composites Part a-Applied Science and Manufacturing*, vol. 37, pp. 858-867, 2006.
[19] G. T. Houlsby and A. M. Puzrin, *Principles of Hyperplasticity*. London: Springer-Verlag London Limited, 2006.
[20] H. Ziegler and C. Wehrli, "The Derivation of Constitutive Relations from the Free-Energy and the Dissipation Function," *Advances in Applied Mechanics*, vol. 25, pp. 183-238, 1987.
[21] A. A. Somashekar, S. Bickerton, and D. Bhattacharyya, "Exploring the non-elastic compression deformation of dry glass fibre reinforcements," *Composites Science and Technology*, vol. 67, pp. 183-200, Feb 2007.